FUNCTIONAL DIAMOND

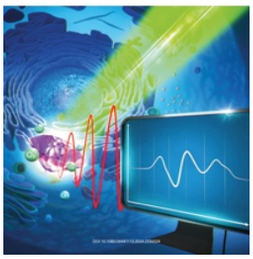

Functional Diamond

ISSN: 2694-1112 (Print) 2694-1120 (Online) Journal homepage: www.tandfonline.com/journals/tfdi20

Production of diamond/Cu composites with high thermal conductivity and low volume fraction using 3D direct ink writing technique

Bingxi Han, Kehao Zhang, Kai Zhang, Mingliang Li & Hailong Wang

To cite this article: Bingxi Han, Kehao Zhang, Kai Zhang, Mingliang Li & Hailong Wang (2026) Production of diamond/Cu composites with high thermal conductivity and low volume fraction using 3D direct ink writing technique, Functional Diamond, 6:1, 2609412, DOI: 10.1080/26941112.2025.2609412

To link to this article: https://doi.org/10.1080/26941112.2025.2609412

Published online: 02 Jan 2026.

FUNCTIONAL DIAMOND
2025, VOL. 6, NO. 1, 2609412
https://doi.org/10.1080/26941112.2025.2609412

Taylor & Francis
Taylor & Francis Group

RESEARCH ARTICLE

OPEN ACCESS Check for updates

Production of diamond/Cu composites with high thermal conductivity and low volume fraction using 3D direct ink writing technique

Bingxi Han, Kehao Zhang, Kai Zhang, Mingliang Li, and Hailong Wang

School of Materials Science and Engineering, Zhengzhou University, Zhengzhou, China

ABSTRACT

Efficient thermal management is critical for the performance and reliability of modern electronic systems. In this study, a pseudoplastic diamond suspension was engineered for DIW and printed into a continuous, 3D-interconnected diamond network, which served as a thermally conductive scaffold. Subsequent infiltration with molten copper enabled full densification of the composite without the need for external pressure. At room temperature, a thermal conductivity of 492.4 ± 20 W/m·K can be achieved at a low diamond loading of 29 vol.%, making a 30.9% enhancement over conventional copper matrix composites containing randomly dispersed diamond particles. This performance is attributed to the continuous and complete 3D diamond framework, which significantly enhances heat transfer while reducing interfacial thermal resistance. The proposed approach provides a new route for the design of diamond metal matrix composites for next-generation thermal management applications.

ABBREVIATIONS

3D: Three dimension; CVD: Chemical vapor deposition; DIW: Direct ink writing; LPBF: Laser powder bed fusion; BJ: Binder jetting; Cu: Copper; PVB: Poly(butyral de vinyle); Cp: Specific heat capacity; α: Thermal diffusivity; ρ: Density; XRD: X-ray diffraction; SEM: Scanning electron microscopy; CT: Computed Tomography; η: Apparent viscosity; κ: Consistency coefficient; τ: Shear stress; τY: Yield stress

ARTICLE HISTORY
Received 8 May 2025
Accepted 22 December 2025

KEYWORDS
Diamond/Cu composites; direct ink writing technology; 3D connected diamond network; heat transfer channel; high thermal conductivity

1. Introduction

With the development of 5 G, artificial intelligence, the demand for increased integration and miniaturization of electronic components has intensified. Consequently, the power density of these components is expected to rise significantly, making efficient thermal management a bottleneck that limits further technological progress. At room temperature, the thermal conductivity of natural diamond can exceed 2240 ± 120 W/m·K, which is the highest thermal conductivity in nature [1–5], and synthetic diamond has the same high thermal conductivity Metal matrix composites with diamond as the reinforcing phase have the advantages of high thermal conductivity and low coefficient of thermal expansion, rendering them highly promising candidates for next-generation thermal management materials [6–12]. Among potential matrix, copper stands out as a cost-effective and low-density alternative to silver, Additionally, copper offers superior thermal conductivity compared to aluminum and does not react with diamond to produce interfacial products that otherwise weaken the overall performance of the composite. Therefore, diamond/copper composites have garnered increasing research attention.

In order to obtain a sufficiently high thermal conductivity, a diamond volume fraction of more than 50 vol% in the composite is essential [13]. However, such high diamond content significantly increases material costs and introduces challenges in processing and machining [13–15]. Thus, a major challenge lies in reducing the diamond content while maintaining excellent thermal conductivity. To address this, increasing attention has been directed toward optimizing the internal heat dissipation architecture to enhance thermal transport efficiency at lower filler loadings. For example, Zhang et al. [13]. prepared 3D interconnected diamond networks in aluminum matrix composites by (chemical vapor deposition) CVD and achieved a thermal conductivity of 315.7 W/m·K at a low diamond loading of 4.6 vol.%. Liu et al. [1]. filled diamond particles into the foam SiC pores to form a 3D-connected reinforced structure, forming a diamond/SiC composite with a thermal conductivity of 298 W/m·K at 26 vol.% diamond loading. Therefore, this gives us the inspiration to construct a three-dimensional interconnected diamond network in a copper matrix to form a heat transfer channel. However, CVD technology for fabricating 3D continuous diamond network is inefficient, time-consuming, and costly. The thermal conductivity of the composites prepared by foaming SiC as

CONTACT Hailong Wang 119whl@zzu.edu.cn

a matrix is still low, highlighting the need for more effective and scalable strategies.

Additive manufacturing technology, which has been developing at a high speed in recent years, provides innovative strategies for the design and fabrication of high-performance composite materials. It is widely recognized as a highly effective approach for producing diamond-reinforced composites with complex geometries. To date, several AM techniques have been utilized in the fabrication of diamond composites, including direct ink writing (DIW), laser powder bed fusion (LPBF), and binder jetting (BJ). For example, Huang et al. explored the fabrication of porous-structured diamond grinding wheels with excellent self-sharpening performance using direct ink writing. In another study [16], Loic Constantin et al. successfully fabricated Cu/5 vol.% diamond composites with a monolithic diamond structure *via* the LPBF process, achieving a thermal conductivity of 349 W/m·K [17]. However, the high-power laser beams used in LPBF processes can cause graphitization of the diamond due to the extreme localized sintering temperatures. Additionally, Ding et al. reported the development of diamond/Cu composites *via* binder jetting, which reached a relative density of 94.6% and a thermal conductivity of 343 W/m·K. The disadvantage of high equipment costs and stringent powder material requirements is shared by both LPBF and BJ techniques [18]. As a type of additive manufacturing technology, 3D direct ink writing is favored due to its low cost, simple device construction, and broad material compatibility. 3D direct ink writing technology, as a manufacturing method based on extruding pseudoplastic inks in layers of poured, stacked molding, is capable of preparing materials with designed microstructures at defined length scales. Therefore, combining the ability of 3D direct ink writing technology to create complex designs with the outstanding properties of diamond/Cu materials can unleash the full power of diamond/Cu materials and reshape its applications [17].

The aim of this study is to obtain diamond/Cu composites with high thermal conductivity at lower diamond loading. A pseudoplastic diamond suspension was configured as a direct-writing ink, enabling the construction of a three-dimensionally interconnected diamond network to serve as an efficient thermal conduction pathway *via* a 3D direct-ink writing technique. The obtained diamond structure was subsequently infiltrated into metallic Cu through a pressureless fusion infiltration process to achieve final densification. Notably, this work represents the first successful application of 3D direct ink writing for the fabrication of diamond/Cu composites. The resulting composites demonstrated a substantial enhancement in thermal conductivity even at low diamond volume loading, significantly outperforming conventional composites reinforced with randomly dispersed diamond particles.

2. Experimental procedures

2.1. Materials

Copper powder (99.9% purity, purchased from Zhongnuo New Material Technology Co., Ltd.) was used as the matrix material, and HPD-C diamond particles were used as the reinforcing phase (particle size of 100–120 μm, purchased from Henan Yellow River Hornet Co., Ltd.) to prepare the composites.200 mesh chrome powder (99.9% purity, purchased from Zhongnuo New Material Technology Co., Ltd.) was used for diamond surface coating. Polyvinyl butyral powder (M.W. 25,000–40,000) was supplied by Shanghai McLean Company (Shanghai, China) for the configuration of DIW ink.

2.2. Preparation

The chrome coating of HPD-C diamond particles was conducted by the vacuum thermal diffusion method. Specifically, using a drum ball mill mixes diamond and chromium powder according to the mass ratio of 1:3 for 30 min. The obtained mixture was heated up to 900 °C at a heating rate of 10 °C/min for 3h under a high vacuum($<10^{-2}$ Pa), and then naturally cooled down room temperature. Subsequently, the sintered samples were ultrasonically cleaned to obtain the high-quality chromium-coated diamond.

The suspension of Cr-coated diamond particles used as DIW ink was configured with a PVB alcohol solution at a concentration of 12% as a binder and a solid content of 65%. A direct ink writing device (Unibuliuder-D300, Youlibide Hangzhou Technology Co., Ltd. Zhejiang, China) was used for 3D printing of diamond network structures. For the printing process, an 18 G dispensing tip was selected, with the printing speed maintained at 20 mm/min, the extrusion pressure controlled within the range of 2.5×10^3–3×10^3 Pa, and the substrate temperature set at 70 °C to facilitate heat-induced curing.

According to the thermal decomposition temperature of PVB, the diamond network is heated to 350 °C at a heating rate of 1 °C/min and then held for 30 min under a nitrogen atmosphere to remove the PVB binder.

Diamond/Cu composites were fabricated using a pressureless molten metal infiltration method. The process was conducted under high vacuum conditions ($<10^{-2}$ Pa), with the temperature ramped to 1200 °C at a rate of 8 °C/min and held for 30 min to ensure complete melting of Cu. Subsequently, the temperature was reduced to 600 °C at a controlled rate of 4 °C/min. A schematic illustration of the overall fabrication procedure is provided in Figure 1.

2.3. Characterization

The microstructures and morphologies of the obtained composites were examined by Cu Ka X-ray diffraction (XRD, Rigaku DMAX-RB, Japan) and field emission

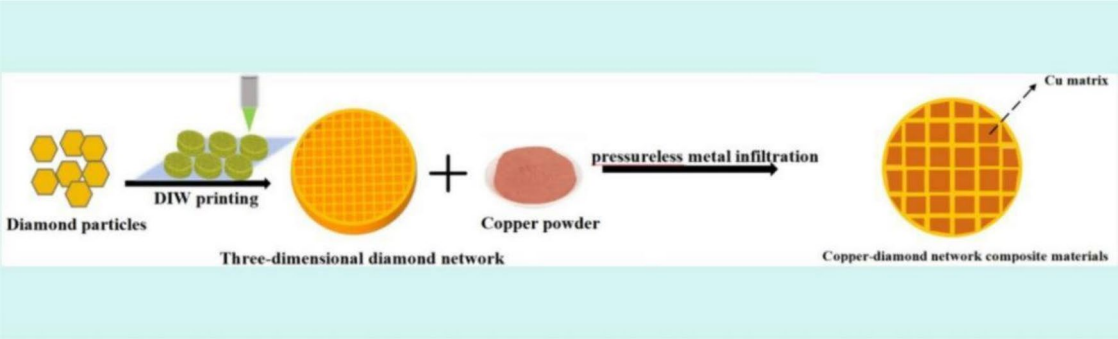

Figure 1. Schematic diagram illustrating the preparation process of diamond/Cu composites *via* the pressureless molten metal infiltration method.

scanning electron microscopy (SEM, ZEISS SIGMA 500, Germany). The rheological properties of diamond particle suspensions were assessed with a rotational rheometer using Anton Paar MCR 302e (Austria) to identify optimal pseudoplastic inks. Steady-state tests at 1 Hz measured apparent viscosity and shear stress from 0.1 to 1000 s^{-1}. And dynamic tests at 10 rad/s determined the storage and loss moduli under shear stresses of 1–10,000 Pa.

The thermal diffusivity (α) was measured using the laser flash method (Netzsch LFA-427, Germany), with an uncertainty of 2.5%. To minimize heat signal reflection and ensure a uniform surface temperature during measurement, prevents the laser pulse from penetrating directly into the sample, which can lead to large measurement errors, the specimen surfaces were coated with a thin layer of carbon spray prior to testing. The density (ρ) was determined by the Archimedes method, with an uncertainty of 1%, and the theoretical density is calculated by the summation rule (rule of mixtures). The specific heat capacity (Cp) was measured using differential scanning calorimetry(Netzsch STA-449F5, Germany), with an uncertainty of 2.5%. The overall uncertainty in the calculated thermal conductivity ($\lambda = \alpha \cdot \rho \cdot Cp$) is estimated to be within 5%. Unless otherwise stated, all measurements were performed at room temperature (25 ± 2 °C). And each measurement was repeated five times to ensure reproducibility.

The internal structure of the composites and the defective condition of the 3D diamond network were characterized by synchrotron radiation computed tomography CT (Phoenix ge V tome S240, UK). The thermal transport properties of the prepared diamond/Cu composites and the reference dispersed diamond-particles/Cu composites, both with identical particle sizes and diamond volume fractions, were evaluated using infrared thermal imaging spectrometer (FOTRIC, China).

3. Results and discussion

3.1. Characterization of Cr-coated diamond

The phase composition of the chromium-plated diamond was characterized by XRD. As shown in Figure 2(a), diamond is the main phase. The diffraction peaks of Cr_3C_2 are more pronounced while the diffraction peaks of Cr_7C_3 are weaker, which suggests that chromium has undergone a chemical reaction on the surface of the diamond, generating Cr_3C_2 and a small amount of Cr_7C_3 on the diamond surface. The surface morphology of chromium-plated diamond is shown in Figure 2(b,c): the coated diamond particles still retained the original cub-octahedral shape with well-defined edges and corners, while continuous and uniform layer of rough chromium carbide coating was formed on the surface of the particles. This coating effectively encapsulated the diamond particles, providing complete surface coverage.

3.2. Direct ink writing of 3D diamond network

The formulation of diamond particle suspensions suitable for 3D direct ink writing is the most important aspect of this study. Particular attention must be given to the rheological properties of the suspension, specifically, its viscosity and yield stress, which are essential for ensuring the printability and structural fidelity of the extruded filaments. In order to obtain suitable ink formulations, the effects of PVB concentration and diamond solid content on the rheological properties were systematically investigated.

Figure 3(a) shows the relationship between shear rate and apparent viscosity for diamond particle suspensions having different PVB alcohol solution concentrations (10 wt.%, 12 wt.%, 14 wt.%, 16 wt.%, 18 wt.%) at a solid content of 50 wt.%. The relationship between shear rate and apparent viscosity can be expressed by the Ostwald-De Waele Model (Equation (1)).

$$\eta = K\dot{\gamma}^{n-1} \tag{1}$$

Which η is the apparent viscosity of the ink; $\dot{\gamma}$ represents the shear rate; K signifies the consistency coefficient, representing the viscosity of the measure, if the viscosity is the higher, the value of K will be greater; n refers to the liquidity index, for the pseudoplasticity of the non-Newtonian fluids, $0 < n < 1$. The fitting results are shown in Figure 3(b–f): the curves conform to the Ostwald-De Waele Model. However, the ink viscosity is low when the concentration of PVB alcohol solution is

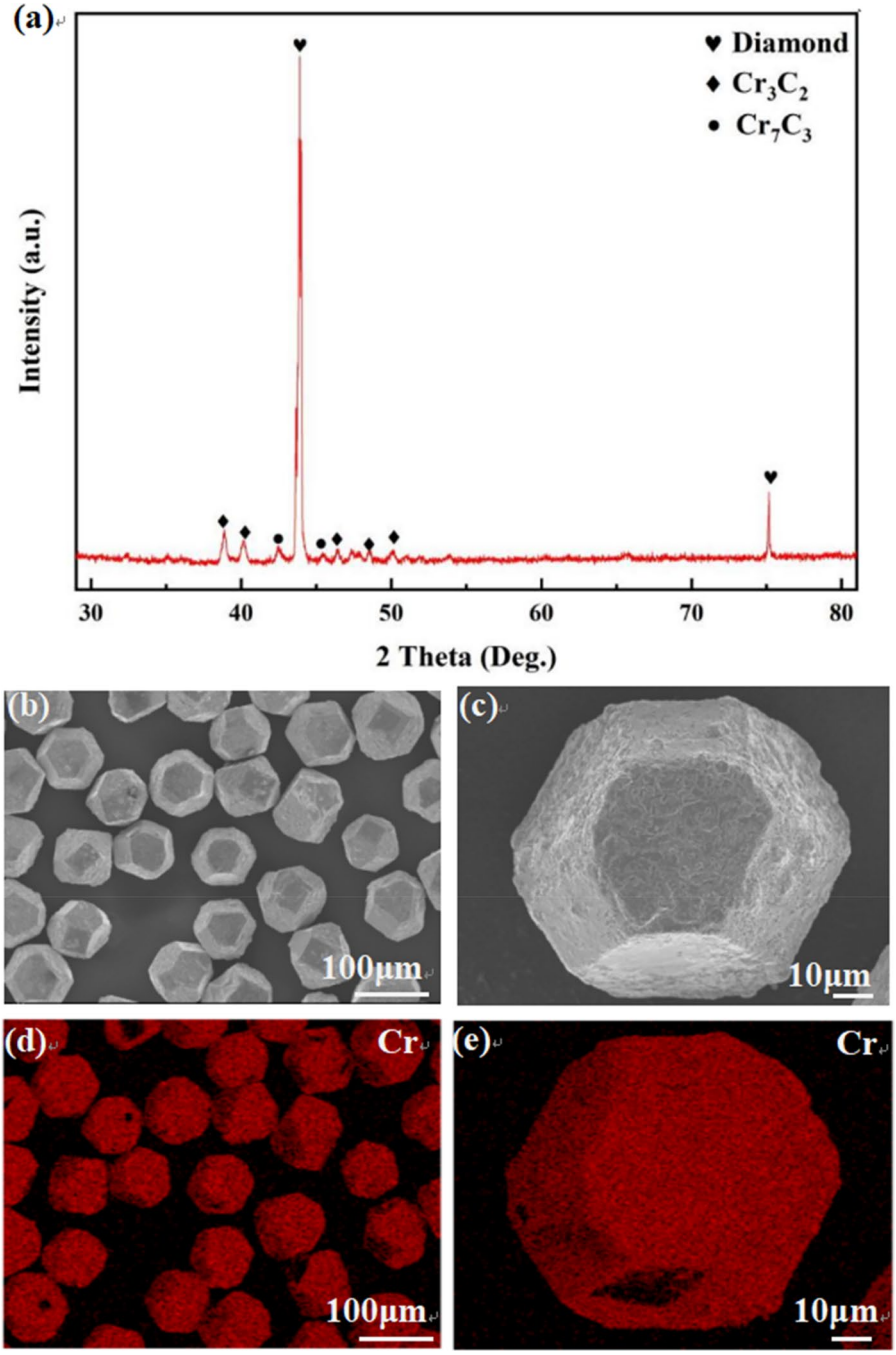

Figure 2. Phase composition and microstructure of Cr-coated diamond: (a) phase composition of Cr-coated diamond; (b,c) surface morphology of Cr-coated diamond at different magnifications; and (d,e) chromium distribution on the surface at different magnifications.

10 wt.%, and the maximum viscosity is about 600 Pa.s. The low-viscosity ink is easy to break up and form secondary droplets when printing, or splash after contacting with the substrate [19], which is not in line with the requirements. In general, the viscosity of DIW inks should be in the range of 6×10^2 to 5×10^5 Pa.s [19]. In addition, the high yield stress ensures that the print filament is self-supporting against gravity and surface tension. The extruded filaments do not collapse or disperse when the applied shear force is withdrawn and maintain their structure until cured. The yield stress of inks is usually limited to the range of 10^2 to 10^3 Pa, which can be obtained by the Herschel–Bulkley model [20,21] (Equation (2)).

$$\tau = \tau_y + \mathrm{K}\dot{\gamma}^n \tag{2}$$

where τ is the shear stress; τ_y represents the yield stress; $\dot{\gamma}$ signifies the shear rate; K is the consistency index and n represents the shear thinning index. The fitting results are shown in Table 1, where R^2 refers to the goodness of fit.

As the concentration of PVB alcohol solution increases, the yield stress first decreases and then increases, and finally reaches 1536.6 ± 79.7 Pa when the concentration of PVB alcohol solution is 18 wt.%. When the PVB content is 10%, the binder is not effective in

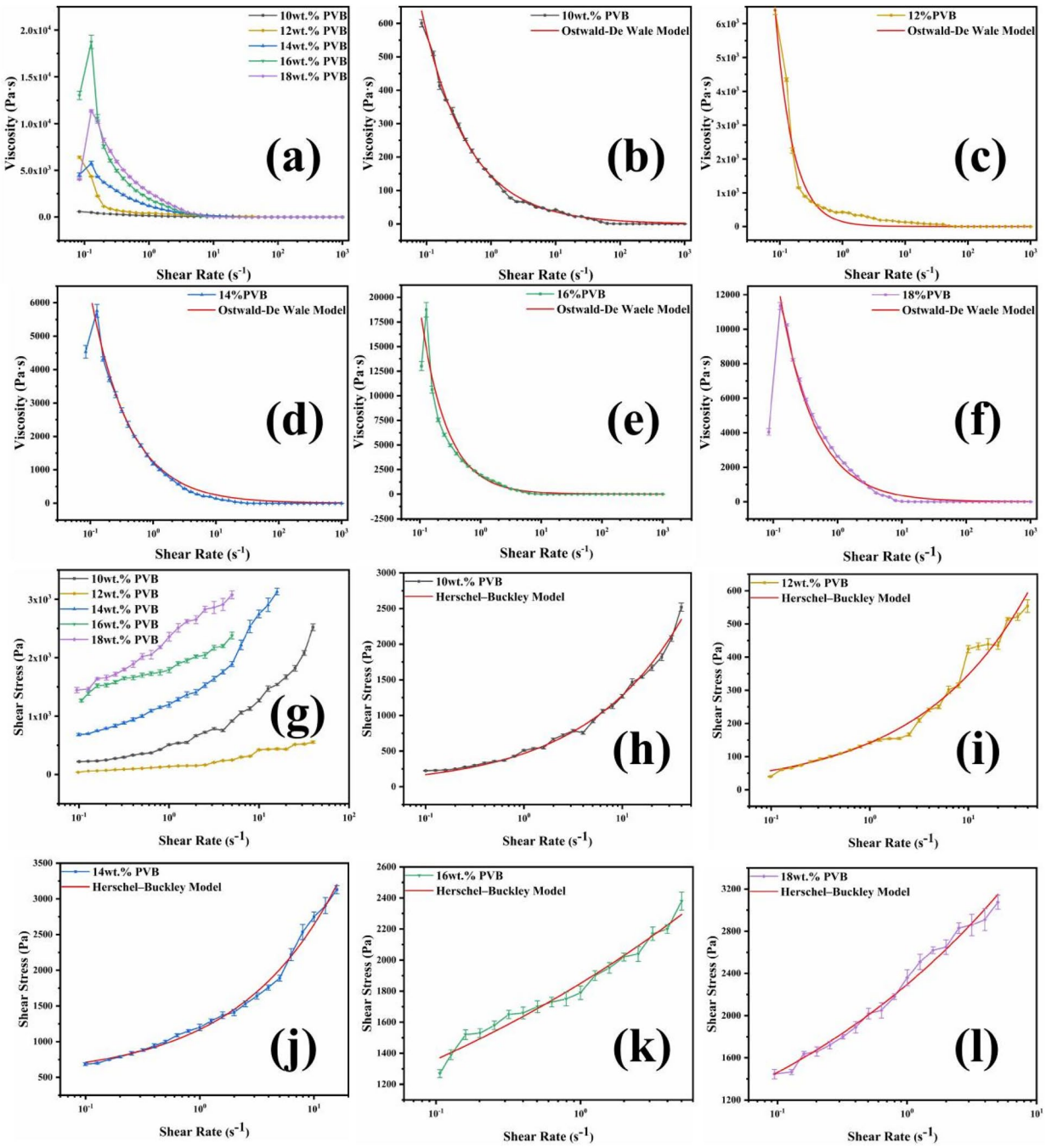

Figure 3. Rheological profiles of diamond particle suspensions having different PVB alcohol solution concentrations at a solid content of 50 wt.%: (a) relationship between shear rate and apparent viscosity; (b–f) results of fitting the Ostwald-De Waele Model; (g) relationship between shear rate and shear stress; and (h–l) results of fitting the Herschel–Bulkley model.

Table 1. Rheological curves of diamond particle suspensions with different PVB alcohol solution concentrations fitted to the Herschel–Bulkley model at 50 wt.% solids content.

The concentration of PVB alcohol solution	n	K (Pa.s^n)	τ_y (Pa)	R^2
10%	0.19 ± 0.01	144.0 ± 7.2	162.9 ± 8.3	0.99 ± 0.05
12%	0.25 ± 0.01	372.9 ± 24.4	44.8 ± 2.1	0.96 ± 0.05
14%	0.38 ± 0.02	673.3 ± 30.6	556.0 ± 33.6	0.97 ± 0.05
16%	0.16 ± 0.01	1352.8 ± 71.4	1298.8 ± 61.9	0.97 ± 0.05
18%	0.30 ± 0.02	2302.7 ± 103.7	1536.6 ± 82.2	0.99 ± 0.05

covering the diamond particles, and particle collisions resulting from Brownian motion lead to aggregation of particles, therefore, which is not adhering to the binder. The yielding behavior of the suspension is governed by the need to overcome interparticle friction. In contrast, an increase in the concentration of the PVB alcohol solution is favorable to improve the coverage of the diamond particle surface, promoting better dispersion and reducing interparticle interactions when a critical concentration is reached. At a critical PVB concentration, a well-dispersed, network-like structure is formed, effectively minimizing particle collisions and resulting in the lowest yield stress. However, further increase in PVB content beyond this point causes flocculation, which leads to increasing yield stress Based on the balance between flowability and structural integrity, a

formulation with a PVB alcohol solution concentration of 14 wt.% and a solid content of 50 wt.% was preferred for subsequent experiments.

As shown in Figure 4, all formulated underwent a transformation of shear thickening, shear refinement, and Newtonian fluid behavior [16]. Specifically, the apparent viscosity increased sharply in the low shear rate region due to shear-induced structuring, then decreased exponentially as shear rate increased, eventually stabilizing at a constant value. This three-stage rheological response was consistent across suspensions with different solid contents, and the apparent viscosity–shear rate curves closely followed the Ostwald-de Waele (power-law) model. In addition, the Herschel–Bulkley model was used to fit the curve of shear stress versus shear rate, and the fitting results are shown in Table 2, where R^2 refers to the goodness of fit.

As the solid content increases, the K value increases, representing an increase in viscosity. This is due to physical cross-linking between more diamond-filled particles and the PVB binder, making the ink more viscous and less fluid. At the same time, when the solid content increases, it corresponds to an increase in the number of diamond particles per unit volume, and the distance between the surfaces of neighboring particles decreases, at which time the PVB chain can only be compressed in order to achieve more diamond particles filled. After the PVB molecular chain is compressed, due to its own

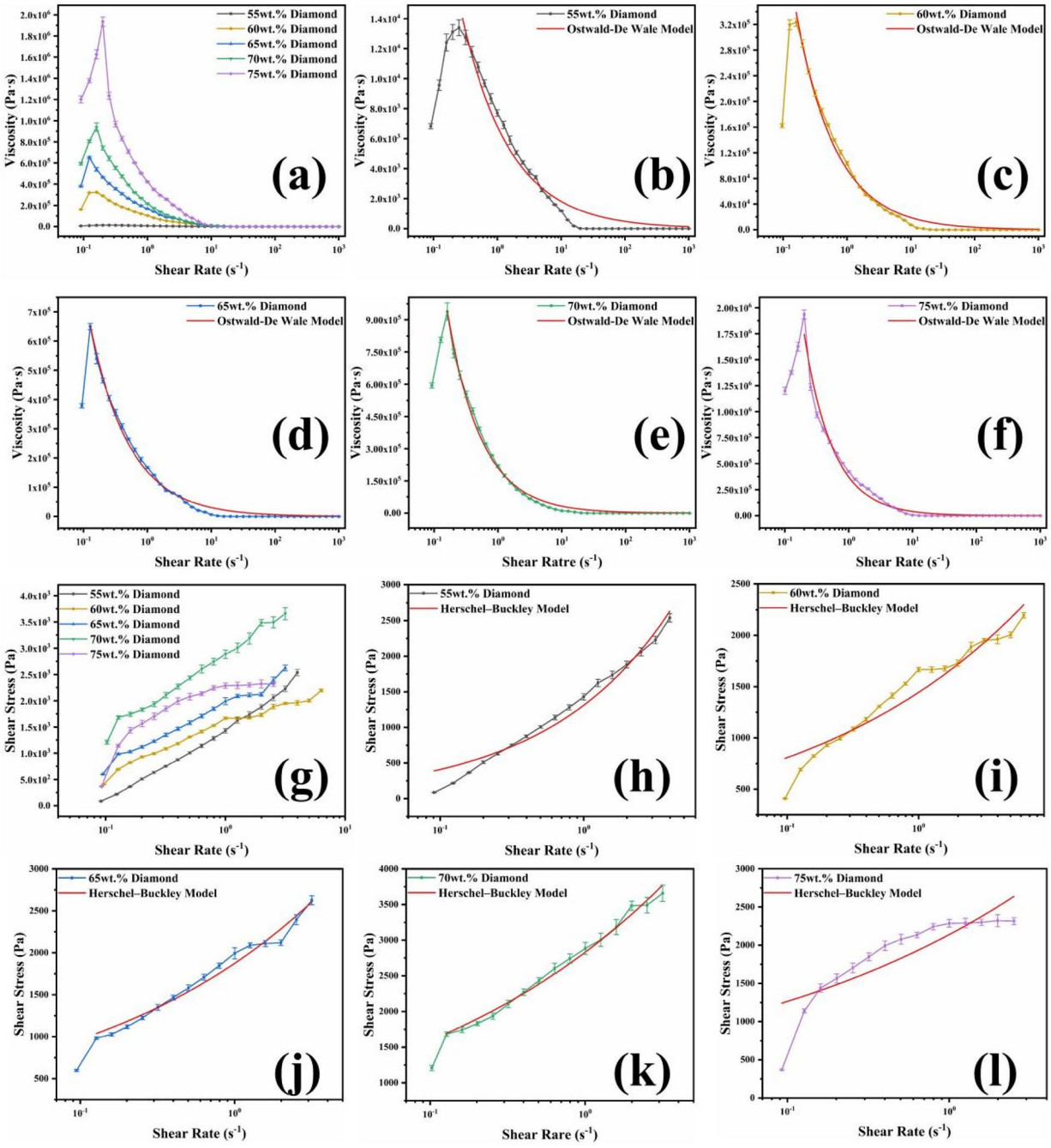

Figure 4. Rheological profiles of diamond particle suspensions with different solid contents at a PVB alcohol solution concentration of 14 wt.%: (a) relationship between shear rate and apparent viscosity; (b–f) results of fitting the Ostwald-De Waele Model; (g) relationship between shear rate and shear stress; and (h–l) results of fitting the Herschel–Bulkley model.

Table 2. Rheological curves of diamond particle suspensions with different solid contents fitted to the Herschel–Bulkley model at a PVB alcohol solution concentration of 14 wt.%.

Solid content	n	K (Pa.s^n)	τ_y (Pa)	R^2
55%	0.26 ± 0.01	1310.4 ± 69.2	253.8 ± 9.1	0.97 ± 0.05
60%	0.32 ± 0.02	1468.7 ± 73.1	784.1 ± 41.5	0.90 ± 0.05
65%	0.50 ± 0.03	1889.1 ± 87.8	892.4 ± 38.9	0.94 ± 0.05
70%	0.64 ± 0.03	2831.5 ± 96.4	1505.3 ± 77.8	0.97 ± 0.05
75%	0.71 ± 0.04	3677.4 ± 196.9	2708.1 ± 99.63	0.66 ± 0.03

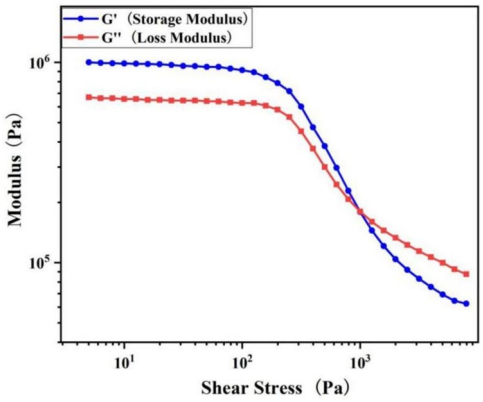

Figure 5. Viscoelastic behavior of diamond particles suspension with PVB alcohol solution concentration of 14 wt.% and 65 wt.% solid content.

elastic recovery effect, it will repel the diamond particles, so that the particles cannot be further close to realize the spatial rearrangement, which is manifested as the yield stress is getting bigger and bigger. When the solid content is 75 wt.%, the yield stress reaches 2708.0 ± 96.9 Pa. At this point, the yield stress is too high causing the ink to be difficult to yield and flow, and there is a significant deviation from the fitted curve. Therefore, the final formula with a PVB alcohol solution concentration of 14 wt.% and a solid content of 65 wt.% was selected for direct-writing 3D printing.

The viscoelastic behavior of the ink under this formulation was evaluated, and the results are shown in Figure 5. The variation of modulus with shear stress corresponds to two curves for storage modulus and loss modulus. The storage modulus is the ability of an ink to store elastic deformation and corresponds to the elastic characteristics of the material. The loss modulus, on the other hand, is the ability of the material to dissipate the deformation and is also known as the viscous modulus, reflecting the viscous characteristics of the material. In the initial linear viscoelastic region, the modulus change is very small and almost constant, which can be regarded as a linear plateau region. With the increase of shear stress, the network of molecular forces within the suspension system is disrupted, and the storage modulus decreases significantly. At higher stress levels, the storage modulus drops below the loss modulus. The intersection of the storage modulus and loss modulus is the point of thixotropy, and the value at this point is approximated as the shear yield stress.

Figure 6(a–e) shows optical photographs of the DIW diamond network after thermal curing at 70 °C for 2 h. The printed sample is a disk with diameter of 30.00 mm, thickness of 3.00 mm and mass of 2.35 g, which is consistent with the design scheme with good structural fidelity and high resolution, indicating that the printing process of the DIW ink is very stable with excellent rheological properties under this formulation. In the mutually orthogonal three-dimensional structural design, the deposited lines are continuously and uniformly arranged as expected, showing no interruption, spreading or deformation phenomena [22], even when passing through the intersection points such as the inflection points, there is no large amount of ink buildup, and the layers are clearly separated from each other, without dispersion or collapse phenomena occurring under the action of gravity and surface tension, exhibiting good self-supporting performance.

Figure 6(f–h) shows localized magnified details of the diamond network obtained by scanning electron microscopy (SEM). The rod-like cylindrical structure can be clearly observed from the magnified image, with high linearity and circularity of the rods [23], no significant difference in the height and thickness of the deposited rods, and no cracks appearing after thermal curing. PVB is uniformly wrapped around the diamond surface to form a coating layer of a certain thickness, which causes the diamond particles to be tightly bonded together at the heat-curing temperature. The fracture surface (Figure 6(i,j)) has the morphology of the binder pulling off, and the presence of PVB can be found on the surface of almost every diamond particle, proving that the PVB adhesive has a high strength and is able to fix the diamond particles firmly.

Figure 7 demonstrates a comparative analysis of the diamond network before and after degreasing, from which the removal of PVB can be clearly seen. Compared with before degreasing, the diamond grains are slightly loosened in stacking, but the diamond particles are still effectively supported due to the retention of part of the thermally cracked carbon. This residual carbon helps maintain the structural integrity of the network, effectively preventing the formation of enlarged interparticle gaps or abnormal pore expansion. Moreover, the low thermal degreasing rate ensures that the shape and dimensions of the printed blanks do not change and that no bulging or cracking occurs. These results confirm the efficacy of the degreasing protocol in preserving both the geometric fidelity and mechanical robustness of the printed diamond structures.

3.3. Thermal conductivity analysis

Figure 8 shows the surface morphology of the diamond/Cu composites under different magnifications, with excellent interfacial bonding between the diamond

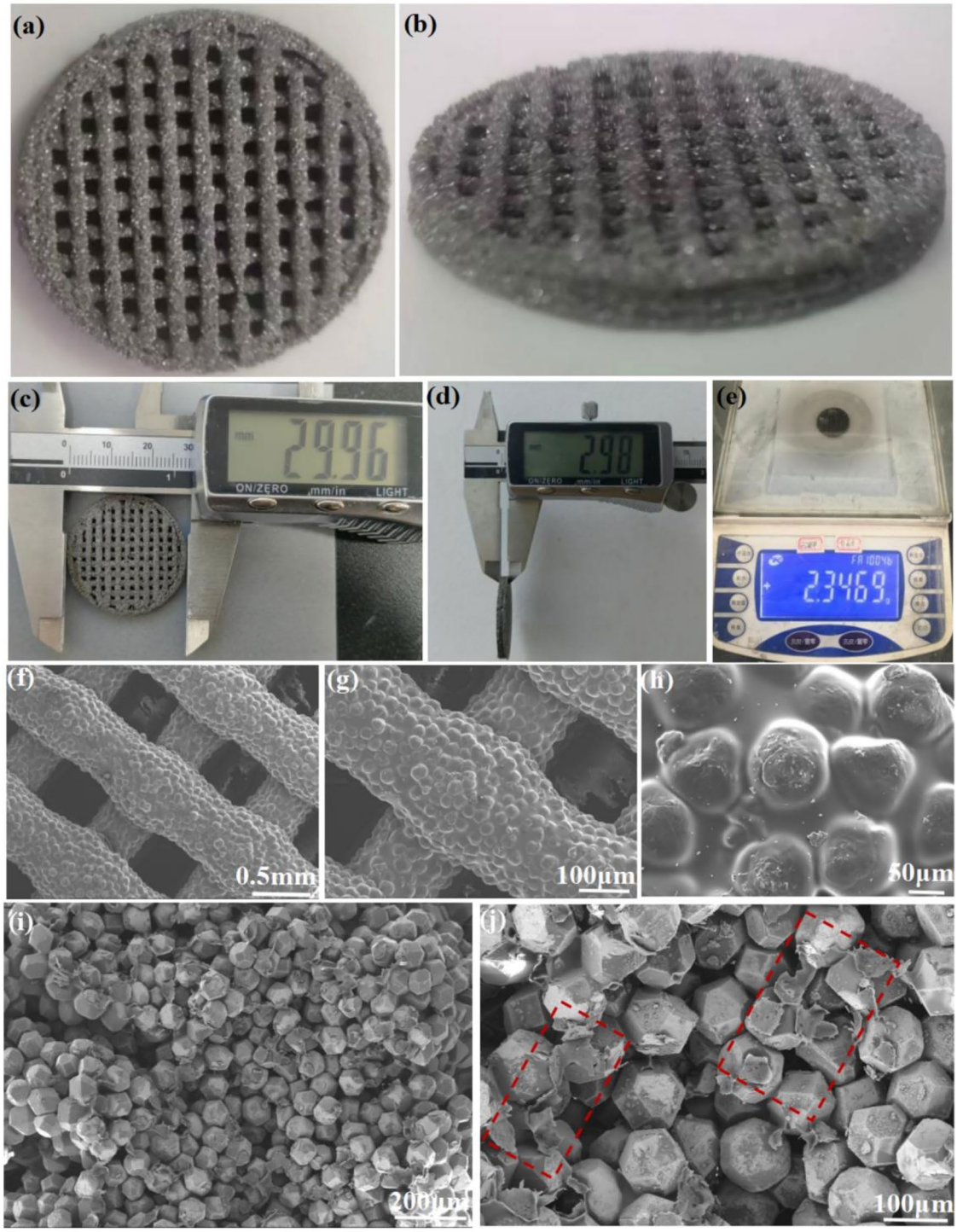

Figure 6. (a–e) Optical photographs of the diamond network after thermal curing; (f–h) surface SEM of the diamond network at different magnifications; and (f–h) cross-section SEM of the diamond network at different magnifications.

particles and the copper matrix, the diamond particles are wrapped in the copper matrix, the copper matrix completely wets the surface of the diamond particles, and the diamond particles and the copper matrix are tightly bonded to each other at the interface, and no obvious interfacial separation phenomenon is observed. This is due to the fact that when using Cr-plated diamond particles, the chromium carbide coating on the surface of the diamond particles improves the sintering characteristics between the diamond particles and the copper matrix, thereby enhancing the interfacial bonding between the diamond particles and the copper matrix. The density of the diamond network/copper composite was measured to be 7.156 g/cm^{-3}, which is comparable to the theoretical density of 7.371 g/cm^{-3}, suggesting that a nearly fully dense composite has been successfully prepared.

It is worth noting that chromium is enriched in the form of fine lines at the interfacial bond between diamond particles and copper matrix (Figure 8(b,f)), while a small portion of chromium is slightly diffused into the copper matrix, and the alloying of copper reduces the

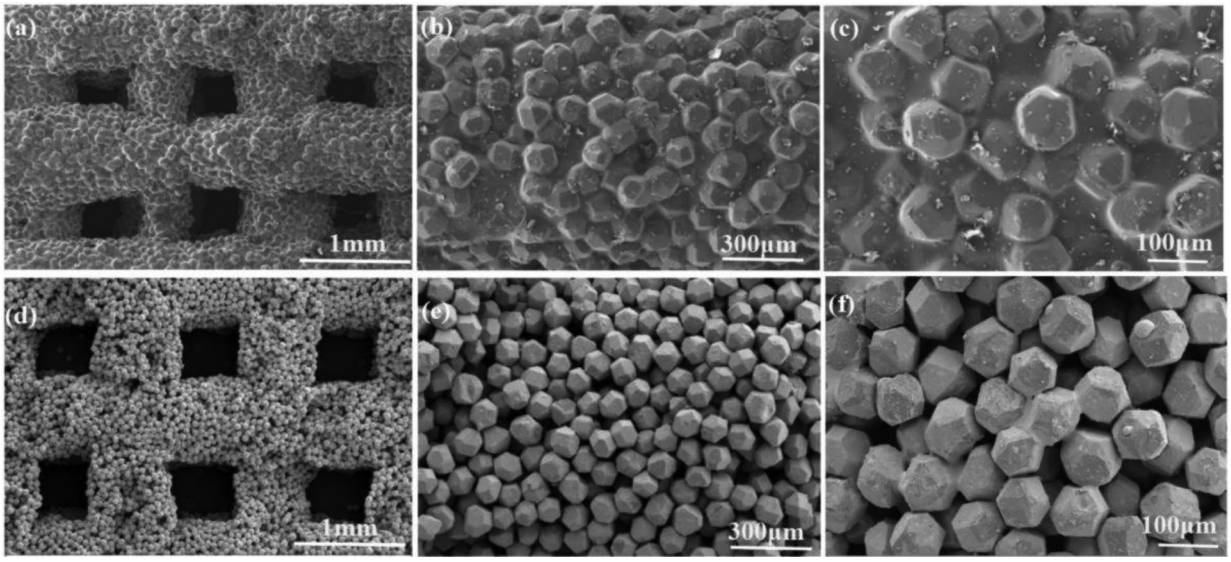

Figure 7. Diamond network before and after degreasing: (a–c) before PVB removal and (d–f) after PVB removal.

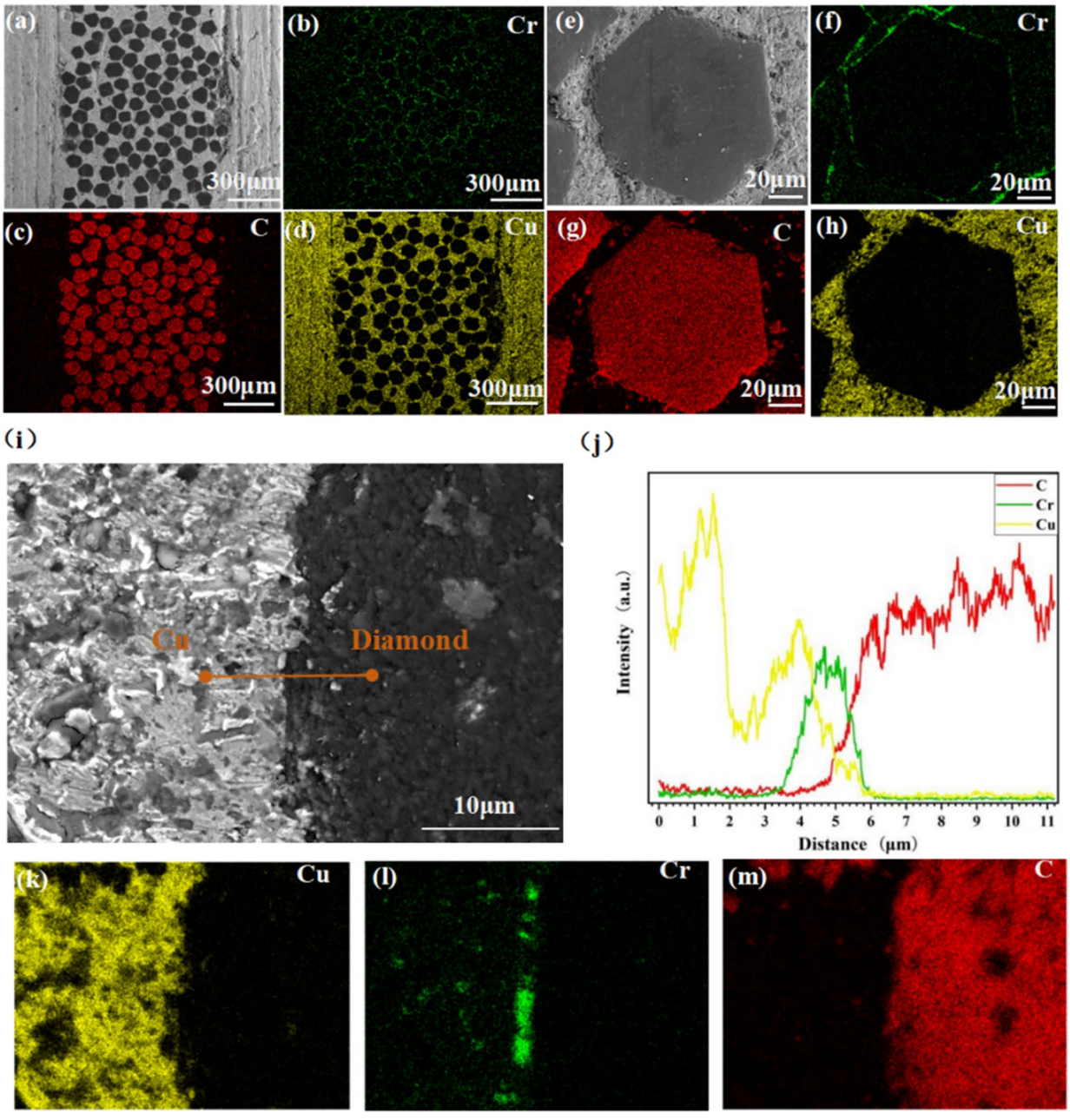

Figure 8. (a–h) SEM images and distribution of elements on the surface of diamond-network/Cu composites at different magnifications; (i) and (k)–(m) test results at the interface between the two phases; and (j) EDS line scan results of the interfacial junction.

thermal conductivity of the copper matrix, which in turn affects the thermal conductivity of the final composite material. Figure 8(i–m) shows the elemental distribution of the diamond/copper composite interfacial bond and the EDS line scan data. As can be seen from the figure: from left to right the interfacial structure undergoes a copper layer-chromium carbide layer-diamond transition in sequence, and the thickness of the chromium carbide layer is measured to be 1.4 μm.

Synchrotron radiation computed tomography provides a powerful non-destructive method for visualizing the true 3D distribution of diamond particles in a copper matrix [24]. A set of different cross sections was randomly intercepted from the measured stereoscopic image CT images of diamond/Cu composites, as shown in Figure 9(c–e). These images reveal that the diamond particles are distributed in the Cu matrix in the form of a network, the diamond network is clear and obvious, and the particles can remain densely connected, and the images of the different CT cross-section layers are basically the same [24]. The entire diamond network was digitally reconstructed from the composite and its three views are shown in Figure 9(f–h). After pressureless infiltration of molten copper, the overall three-dimensional diamond network produced by 3D direct ink writing technique remained continuous and intact, with essentially no defects.

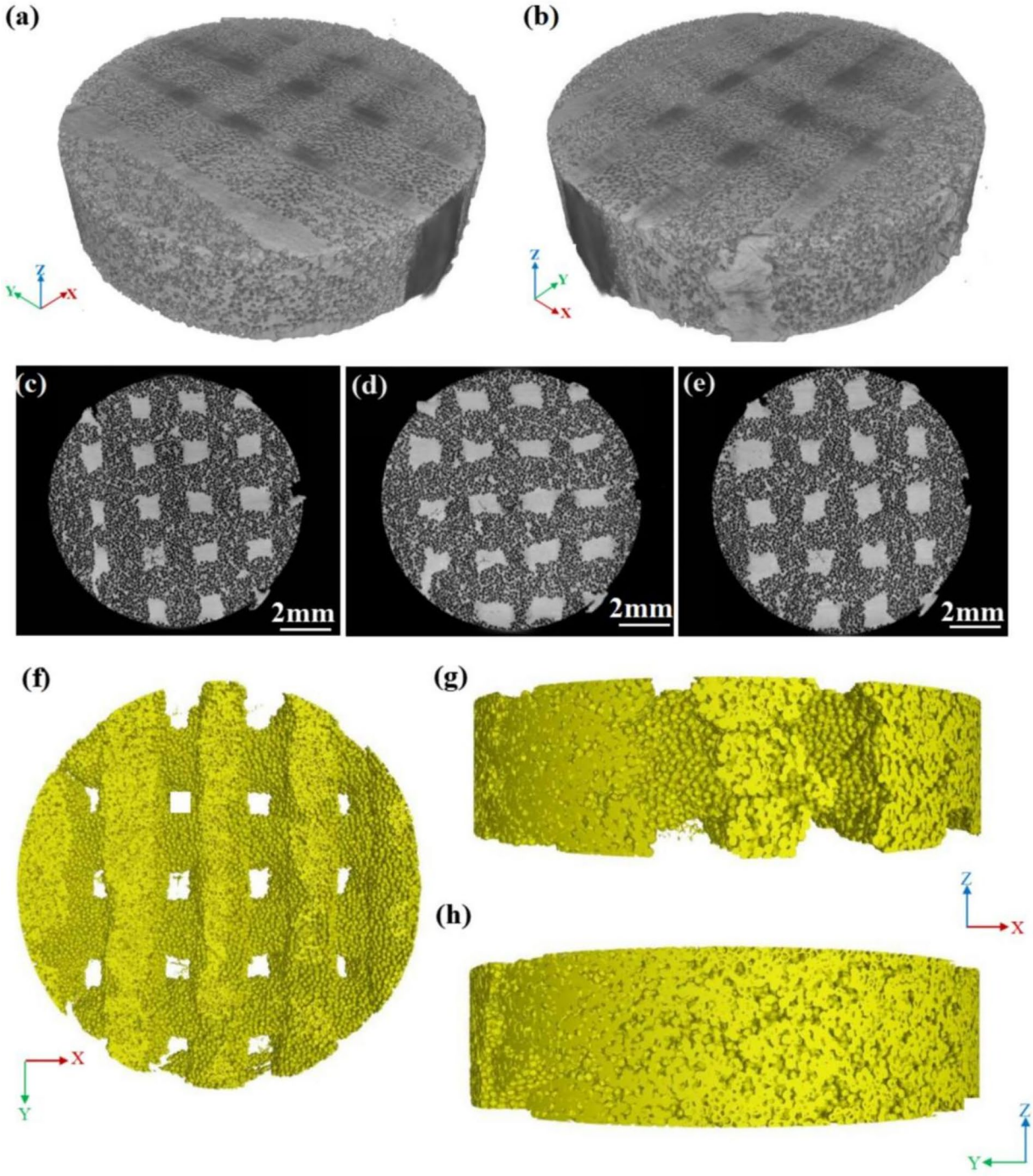

Figure 9. Computed tomography CT images of DN/Cu composites: (a,b) 3D images of the DN/Cu composites as a whole; (c–e) cross-sections of randomly acquired; and (f–h) three-views of the extracted diamond particles.

After weighing the same mass of Cr-coated diamond particles and mixing them with high-purity copper powder in a roller ball mill, diamond-particles/Cu composites of the same dimensions (30.3 mm in diameter and 3.1 mm in thickness) were prepared using the same sintering process, and the thermal conductivity was measured to be 376.2 W/m·K. Compared to the composites with dispersed diamond particles, the thermal conductivity of the composites with diamond particles printed into three-dimensional diamond networks by the DIW technique is 492.4 W/m·K, which is a 30.9% increase in thermal conductivity.

To provide a more intuitive comparison of the heat transfer capacity between two samples, an infrared thermal imaging spectrometer was used to record the top surface infrared images and temperature changes [13], the results of which are shown in Figure 10. The two samples were placed on a hot plate at a constant temperature of 100 °C during the heating stage, and when heated to the 10th s, the temperature of the top surface of the dispersed diamond-particles/Cu composites increased by 15.8 °C, whereas the diamond/Cu composites reached a significantly higher surface temperature of 26.4 °C. Within the temperature range of 24 °C to 80 °C, the heating rate of dispersed diamond-particles/Cu composites was 0.8 °C/min, while diamond/Cu composite was 1.1 °C/min, which was 1.3 times higher.

Both samples were fully heated at 80 °C for 30 min during the cooling phase and subsequently transferred to a room-temperature plate to initiate the cooling phase. The dispersed diamond-particles/Cu composites took 127s to reach room temperature, and the diamond/Cu composites took 100s, reflecting a 27% reduction in cooling time. During heating and cooling, the top

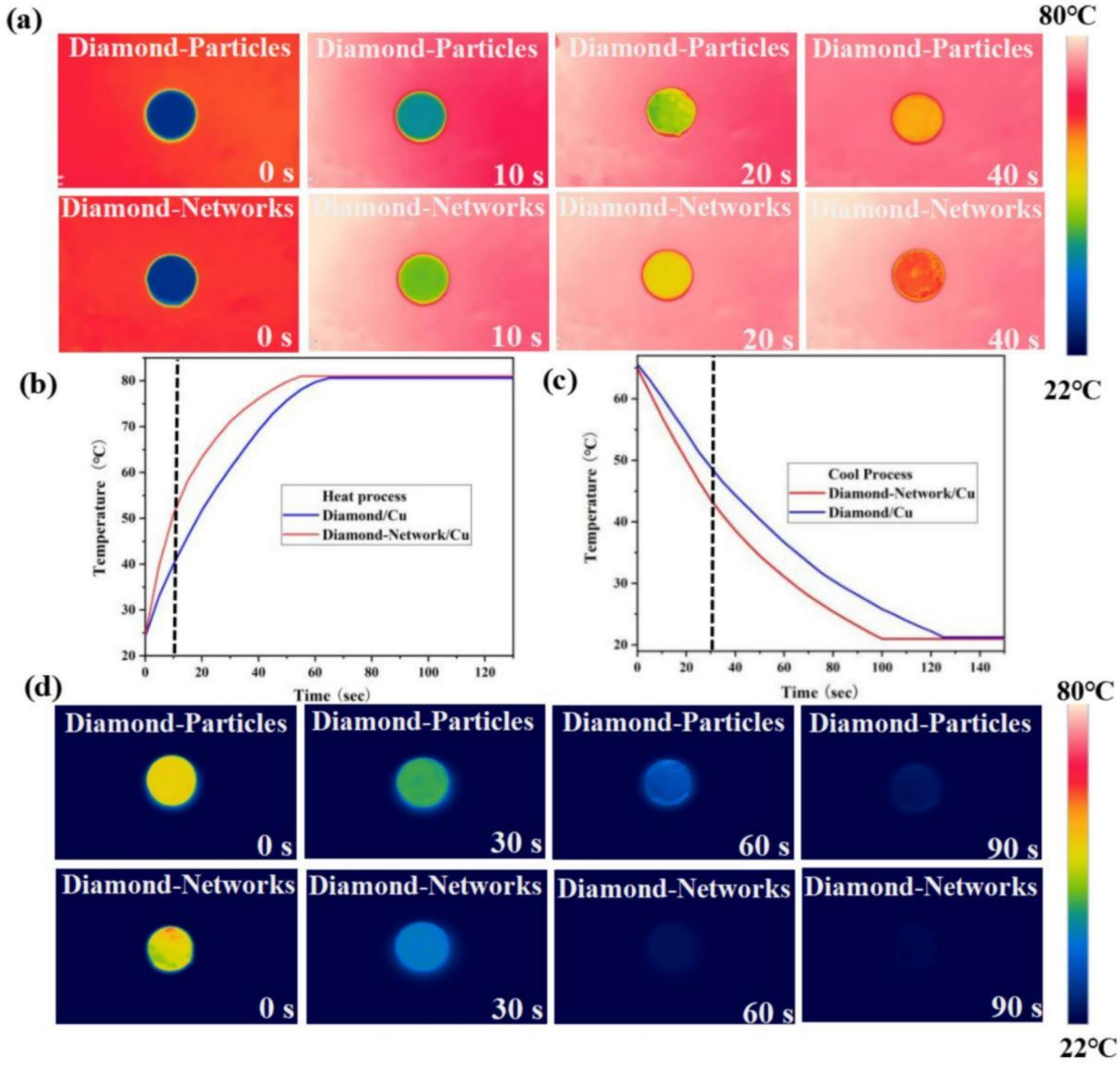

Figure 10. Infrared thermography characterization of diamond/Cu composites and diamond-particles/Cu composites and the corresponding heating and cooling curves: (a) infrared camera image of the heating stage; (b) curve of the top surface temperature versus the heating time; (c) curve of the top surface temperature versus the heating time; and (d) infrared camera image of the cooling stage.

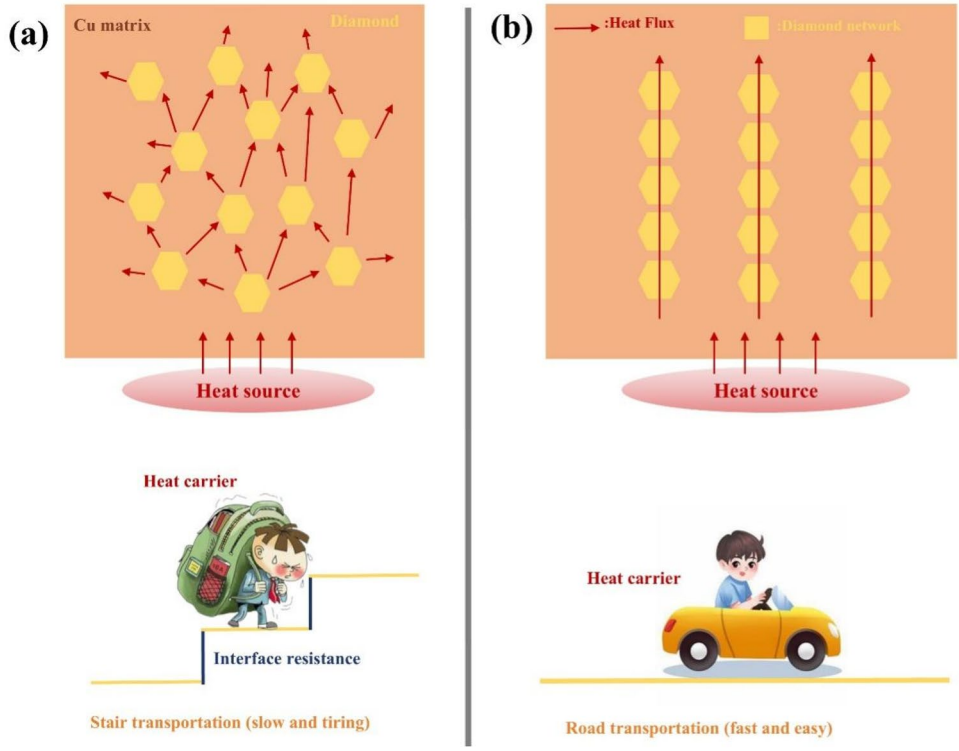

Figure 11. Comparison of heat transfer models of diamond/Cu composites and diamond-particles/Cu composites: (a) heat transfer model of Cu matrix composites reinforced by dispersed diamond particles and (b) heat transfer model of Cu matrix composites reinforced by 3D connected diamond network.

surface temperature and the relative infrared thermal images of the diamond/Cu composites changed more rapidly than those of the composites prepared with dispersed diamond particles [25], and the temperature response was basically consistent with the thermal diffusivity, further validating the effectiveness of the enhanced thermal conductivity of the three-dimensional diamond network.

The comparative heat transfer model in Figure 11 explains the superiority of the 3D connected diamond network. In diamond/copper composites, the thermal conductivity of the copper matrix is mainly through the free movement of through the free movement of outer-layer electrons. In contrast, heat transfer within the diamond reinforcement, being a non-metallic crystal, occurs *via* lattice vibrations, known as phonon-mediated conduction. Due to the different thermal conductivity mechanisms between the copper matrix material and the diamond reinforcement, the interfacial bond creates a great interfacial resistance that hinders heat transfer. If the diamond particles are dispersed in the copper matrix, the heat flux must repeatedly overcome interfacial resistance as it crosses each diamond-copper interface, making heat transfer inefficient. However, by connecting isolated diamonds to form a three-dimensional diamond network, a highly efficient heat transfer pathway is constructed inside throughout the copper matrix, and heat flow can be transmitted more efficiently and quickly through the new path without resistance. At the macroscopic level, this structural enhancement is reflected in a significant increase in thermal conductivity [1,13,26].

4. Conclusions

In this work, we demonstrated that constructing a three-dimensional interconnected Cr-coated diamond network and integrating it into a copper matrix *via* pressureless infiltration can effectively enhance both structural integrity and interfacial compatibility in diamond/copper composites. The continuous 3D diamond architecture was shown to serve as an efficient heat-conduction pathway, markedly reducing interfacial thermal resistance and enabling superior thermal transport compared with composites reinforced with randomly dispersed diamond particles. The study highlights the importance of network architecture in determining the thermal performance of metal matrix composites and provides valuable insights into the design principles for next-generation high-performance thermal management materials. Overall, the findings establish a clear link between microstructural design and functional performance, offering a practical strategy for engineering advanced diamond/metal systems with optimized thermal conductivity.

Disclosure statement

No potential conflict of interest was reported by the author(s).

Funding

This study was supported by National Natural Science Foundation of China (No. 52172075), the Project of Zhongyuan Critical Metals Laboratory (No. GJJSGFJQ202303), and Sanmenxia Major Science and Technology Project (No. 2022001003).

Notes on contributors

Bingxi Han is a master student at Zhengzhou University. His research focuses on the design and fabrication of diamond/Cu composites with high thermal conductivity using three-dimensional direct ink writing (3D-DIW) techniques.

Dr. Kehao Zhang is currently affiliated with the School of Materials Science and Engineering at Zhengzhou University. His primary research focuses on environmental functional ceramics and thermal management materials.

Kai Zhang is a Ph.D. student at Zhengzhou University. His research focuses on the thermal conductivity of diamond/Cu composites, with particular emphasis on interfacial heat transport, microstructural optimization, and composition-property relationships.

Dr. Mingliang Li is an Associate Professor at Zhengzhou University. His current research interests focus on the synthesis and processing of high-entropy ceramics, with particular emphasis on tailoring their microstructures to achieve enhanced mechanical properties and multifunctional properties, such as improved thermal, electrical.

Prof. Dr. Hailong Wang is a Full Professor at the School of Materials Science and Engineering, Zhengzhou University, China, where he earned his Ph.D. in Physics in 2007. He has published over 260 papers in peer-reviewed journals and has been recognized among the Top 2% of Scientists Worldwide. His current research interest is focused on two research areas, namely (i) high-entropy ceramics with ultrahard and wear-resistant properties as well as (ii) the design of advanced structural and functional ceramics for ultra-high temperature applications.

References

[1] Liu P, He X, Qu X. Preparation of high thermal conductivity diamond/SiC composites with 3D connected diamond at low volume fraction. Compos Commun. 2023;39:101526. doi: 10.1016/j.coco.2023.101526

[2] Berman R, Hudson PRW, Martinez M. Nitrogen in diamond: evidence from thermal conductivity. J Phys C Solid State Phys. 1975;8(21):L430–L434. doi: 10.1007/978-1-4899-3751-3_1

[3] Liu C, Lu P, Chen W, et al. Phonon transport in graphene based materials. Phys Chem Chem Phys. 2021;23(46):26030–26060. doi: 10.1039/D1CP02328D

[4] Niyikiza AB, Xiang Z, Zhang F, et al. Thermal conductivity of boron arsenide above 2100 watts per meter per Kelvin at room temperature. Mater Today. 2025;90:11–14. doi: 10.1016/j.mattod.2025.09.021

[5] Inyushkin AV, Taldenkov AN, Ralchenko VG, et al. Thermal conductivity of pink CVD diamond: influence of nitrogen-related centers. J Appl Phys. 2023;133(2):025102. doi: 10.1063/5.0115623

[6] Abyzov AM, Shakhov FM, Averkin AI, et al. Mechanical properties of a diamond–copper composite with high thermal conductivity. Mater Des. 2015;87:527–539. doi: 10.1016/j.matdes.2015.08.048

[7] Bai H, Ma N, Lang J, et al. Effect of a new pretreatment on the microstructure and thermal conductivity of Cu/diamond composites. J Alloys Compd. 2013;580:382–385. doi: 10.1016/j.jallcom.2013.06.027

[8] Rape A, Gott K, Kulkarni A, et al. Simulation of matrix conductivity in copper–diamond composites sintered by field assisted sintering technology. Comput Mater Sci. 2015;110:29–33. doi: 10.1016/j.commatsci.2015.07.030

[9] Shen X-Y, He X-B, Ren S-B, et al. Effect of molybdenum as interfacial element on the thermal conductivity of diamond/Cu composites. J Alloys Compd. 2012;529:134–139. doi: 10.1016/j.jallcom.2012.03.045

[10] Xie Z, Guo H, Zhang X, et al. Enhancing thermal conductivity of diamond/Cu composites by regulating distribution of bimodal diamond particles. Diamond Relat Mater. 2019;100:107564. doi: 10.1016/j.diamond.2019.107564

[11] Zain-Ul-Abdein M, Raza K, Khalid FA, et al. Numerical investigation of the effect of interfacial thermal resistance upon the thermal conductivity of copper/diamond composites. Mater Des. 2015;86:248–258. doi: 10.1016/j.matdes.2015.07.059

[12] Zhang C, Wang R, Cai Z, et al. Effects of dual-layer coatings on microstructure and thermal conductivity of diamond/Cu composites prepared by vacuum hot pressing. Surf Coat Technol. 2015;277:299–307. doi: 10.1016/j.surfcoat.2015.07.059

[13] Zhang L, Wei Q, An J, et al. Construction of 3D interconnected diamond networks in Al-matrix composite for high-efficiency thermal management. Chem Eng J. 2020;380:122551. doi: 10.1016/j.cej.2019.122551

[14] Yang Z, He X, Wu M, et al. Fabrication of diamond/SiC composites by Si-vapor vacuum reactive infiltration. Ceram Int. 2013;39(3):3399–3403. doi: 10.1016/j.ceramint.2012.08.084

[15] Zheng W, He X, Wu M, et al. Preparation and thermal conductivities of diamond/SiC composites. Appl Phys A. 2018;124(12):804–816. doi: 10.1007/s00339-018-2232-y

[16] Huang J, Lu J, Wang Y, et al. Fabrication of porous structure vitrified bond diamond grinding wheel via direct ink writing. Ceram Int. 2021;47(24):34050–34058. doi: 10.1016/j.ceramint.2021.08.314

[17] Constantin L, Kraiem N, Wu Z, et al. Manufacturing of complex diamond-based composite structures via laser powder-bed fusion. Addit Manuf. 2021;40:101927. doi: 10.1016/j.addma.2021.101927

[18] Ding M-M, Fu H, Tian Y-F, et al. Shape, microstructure and properties of diamond/copper composites prepared by binder jet additive manufacturing. Int J Refract Met Hard Mater. 2025;130:107148. doi: 10.1016/j.ijrmhm.2025.107148

[19] Feng J, Su B-L, Xia H, et al. Printed aerogels: chemistry, processing, and applications. Chem Soc Rev. 2021;50(6):3842–3888. doi: 10.1039/C9CS00757A

[20] Khecho A, Ghaffari SA, Eftekhari Yekta B. The influence of particle size distribution on rheological properties of fused silica pastes for direct ink writing. Int J Appl Ceramic Tech. 2022;19(5):2472–2479. doi: 10.1111/ijac.14109

[21] Sun Y, Peng C, Wang X, et al. Rheological behavior of Al2O3 suspensions containing polyelectrolyte complexes for direct ink writing. Powder Technol. 2017;320:223–229. doi: 10.1016/j.powtec.2017.07.049

[22] Li J-J, Li B, Peng Q-M, et al. Fabrication and characterization of direct-written 3D TiO2 woodpile electromagnetic bandgap structures. Chin Phys B. 2014;23(9):502–508. doi: 10.1088/1674-1056/23/9/098104

[23] Liao J, Chen H, Luo H, et al. Direct ink writing of zirconia three-dimensional structures. J Mater Chem C. 2017;5(24):5867–5871. doi: 10.1039/C7TC01545C

[24] Tan Z, Xiong D-B, Fan G, et al. Enhanced thermal conductivity of diamond/aluminum composites through tuning diamond particle dispersion. J Mater Sci. 2018;53(9):6602–6612. doi: 10.1007/s10853-018-2024-y

[25] Xiao C, Chen L, Tang Y, et al. Three dimensional porous alumina network for polymer composites with enhanced thermal conductivity. Compos Part A Appl Sci Manuf. 2019;124:105511. doi:10.1016/j.compositesa.2019.105511

[26] Xiaopeng H, Ying H, Jiaming W, et al. Fabrication of graphite films/copper composites by vacuum hot pressing for high-efficiency thermal management property. Compos Commun. 2021:24:100665–100671. doi: 10.1016/J.COCO.2021.100665